Binding and Interaction of Dinitroanilines with Apicomplexan and Kinetoplastid α-Tubulin

Arpita Mitra[†,‡] and David Sept*[,‡,§]

Department of Chemical Engineering, Center for Computational Biology, and Department of Biomedical Engineering, Washington University, St. Louis, Missouri 63130-4899

Received April 21, 2006

Despite years of use as commercial herbicides, it is still unclear how dinitroanilines interact with tubulin, how they cause microtubule disassembly, and why they are selectively active against plant and protozoan tubulin. In this work, through a series of computational studies, a common binding site of oryzalin, trifluralin, and GB-II-5 on apicomplexan and kinetoplastid α-tubulin is proposed. Furthermore, to investigate how dinitroanilines affect tubulin dynamics, molecular dynamics simulations of *Leishmania* α-tubulin with and without a bound dinitroaniline are performed. The results obtained provide insight into the molecular mechanism by which these compounds interact with tubulin and function to prevent microtubule assembly. Finally, to aid in the design of effective parasitic microtubule inhibitors, several novel dinitroaniline analogues are evaluated. The location of the binding site and the relative binding affinities of the dinitroanilines all agree well with experimental data.

Introduction

Microtubules (MTs[a]) are cylindrical polymers formed by the polymerization of α*β*-tubulin heterodimers. MTs are essential in a diverse array of eukaryotic cell functions, such as mitosis, cell motility, and intracellular organelle transport. Many of these cellular processes are associated with the dynamic reorganization of MT arrays, which is often regulated by the interaction of various small molecules and accessory proteins with the tubulin dimer or microtubules. Dinitroanilines are widely used in herbicide formulations because they bind with high affinity to plant tubulin, inhibit tubulin assembly, and disrupt MTs of plants.[1−3] Interestingly, these compounds also inhibit parasite growth and differentiation as well as depolymerize MTs of parasitic protozoa, such as *Trypanosoma* spp.,[4,5] *Leishmania* spp.,[6−8] *Plasmodium falciparum*,[9] and *Toxoplasma gondii*.[10] In contrast, dinitroanilines are ineffective against mammalian and fungal tubulin.[7,11] This selective activity of the dinitroanilines against parasitic tubulin gives them the potential of being developed as anti-parasitic agents. For this reason, molecular characterization and structure−activity relationship data is required to design dinitroaniline analogues for use as effective therapeutic agents against life-threatening infectious diseases, such as leishmaniasis, trypanosomiasis, toxoplasmosis, and malaria.

The flagellate protozoan parasite *Leishmania* spp. belongs to the phylum Kinetoplastida and causes visceral and cutaneous leishmaniasis in humans. The dinitroaniline **1** (oryzalin; see Figure 1) inhibits the polymerization of partially purified *Leishmania* tubulin resulting in abnormal MTs, whereas rat brain tubulin polymerizes normally.[11] Compound **2** (trifluralin), an analogue of **1**, binds selectively to partially purified *Leishmania* spp. tubulin as compared to rat brain tubulin.[7] More recently, **3** (GB-II-5), which differs from **1** in having a phenyl ring at the *N1* nitrogen of the sulfonamide, has been shown to be more potent and likewise have selective activity against *Leishmania* tubulin polymerization.[12] **3** binds 11-fold stronger to *Leishmania* tubulin than **1**, and at concentrations below where **3** completely inhibits the polymerization of *Leishmania* tubulin, porcine brain tubulin is inhibited by only 17%.[13]

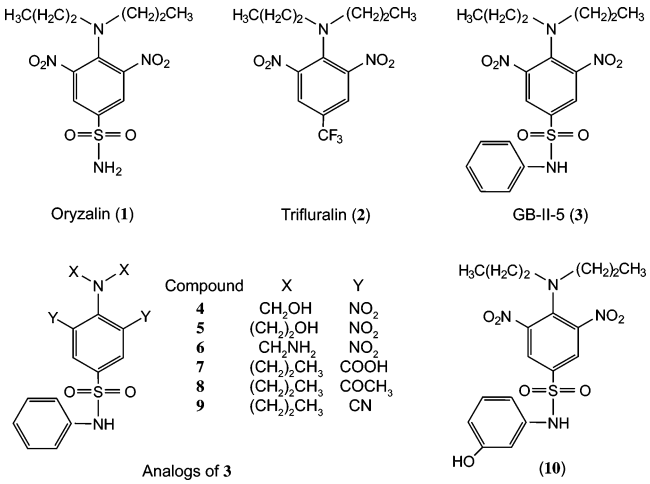

Figure 1. Structures of all dinitroaniline analogues used in docking and simulation studies.

The obligate intracellular parasites such as *Toxoplasma gondii* and *Plasmodium falciparum* belong to the phylum Apicomplexa. Infection by *T. gondii* can result in miscarriage, birth defects in newborns, or the loss of vision in immunocompetent hosts as well as toxoplasmic encephalitis in HIV-infected individuals. *P. falciparum* parasites cause the most lethal form of human malaria, which is responsible for over a million deaths a year. **2** binds selectively to *Plasmodium* tubulin and induces the disassembly of subpellicular MTs in *P. falciparum* gametocytes and merozoites.[14,15] Interestingly, **1** displays 10-fold higher activity than **3** against *P. falciparum* (Werbovetz, K. Personal communication), whereas *T. gondii* tachyzoites are more sensitive to **1** than **3** (Morrissette, N. Personal communication).

Recently, 23 *Toxoplasma* α-tubulin mutations associated with resistance to **1** were identified and characterized.[16] These results provided strong evidence that **1** binds to α-tubulin; however, many of these mutations were located in the core of α-tubulin,

* To whom correspondence should be addressed. Tel: 314-935-8837. Fax: 314-935-7448. E-mail: dsept@biomed.wustl.edu.
† Department of Chemical Engineering.
‡ Center for Computational Biology.
§ Department of Biomedical Engineering.

[a] Abbreviations: MT, microtubule; MD, molecular dynamics; R_g, radius of gyration; rmsf, root-mean-square fluctuations.

10.1021/jm060472+ CCC: $33.50
Published on Web 07/28/2006

indicating that their effect was probably allosteric. Solely on the basis of these genetic studies, a binding location for **1** on *Toxoplasma* α-tubulin could not be identified. However, by combining this work with computational studies, we were able to localize the binding to a specific site on α-tubulin. In the current work, we have expanded upon our previous results[16] and examined several dinitroanilines and their interactions with *Leishmania*, *Toxoplasma*, and *Plasmodium* α-tubulin. We have also performed molecular dynamics simulations of the *Leishmania* α-tubulin−**3** complex to determine the molecular function of these compounds. Finally, to aid in the design of effective parasitic MT inhibitors, analogues of **3** with substitutions in the aryl ring at the *N1* nitrogen, as well as modifications at the *N4* nitrogen and at the nitro groups present on the sulfanilamide ring were evaluated.

Materials and Methods

Preparation of Ligands and Protein Structures. Ligands **1**−**10** (Figure 1) were constructed as all-atom entities, energy minimized using the Tripos force field, and assigned partial atomic charges based on the Gasteiger−Marsili method using Sybyl v6.8 (Tripos Inc., St. Louis, MO).

The electron crystallographic structure of the bovine tubulin heterodimer (pdb entry: 1JFF) was completed as described previously.[16] This structure was then used as a homology model template to create the structure of *T. gondii* α-tubulin (accession code: AAA30145). Because the two α-tubulin sequences are 84% identical, the *Toxoplasma* sequence was threaded on to the 1JFF structure, and the differing amino acid side chains were modeled in using WHAT-IF.[17] Similarly, *P. falciparum* and *L. major* α-tubulin share 93% and 86% sequence identity, respectively, with *T. gondii* α-tubulin. Hence, the *Toxoplasma* α-tubulin structure was used as a homology model template for *P. falciparum* (accession code: CAA34101) and *L. major* (accession code: CAJ02501) α-tubulin structures, using the same procedure described above.

To determine the binding site of the dinitroanilines, ensembles of conformations for *Toxoplasma*, *Plasmodium*, and *Leishmania* α-tubulin were required. Using the molecular dynamics (MD) program NAMD v2.5,[18] simulations of the parasitic α-tubulin−GTP complexes were performed using the isothermal-adiabatic (NPT) ensemble with CHARMM27 force field and TIP3P model for water. Interactions were evaluated on the basis of a multiple-time stepping algorithm, where the bonded interactions (using SHAKE algorithm) were computed every 2 fs, the short-range nonbonded electrostatic and van der Waals interactions (10 Å cutoff with a smooth switching function beginning at 8.5 Å, and pairlist distance of 11.5 Å) every 2 fs, and the long-range electrostatic interactions every 4 fs. Particle-Mesh Ewald was used to compute the long-range electrostatics with grid points at least 1 Å in all directions. NPT simulations were performed at 1 atm using a Nosé-Hoover Langevin piston with a decay period of 200 fs and a damping time scale of 100 fs (for heating and equilibration phases) and 500 fs (for production phase), coupled with temperature control involving Langevin dynamics. The steps of the MD simulations included energy minimization down to a gradient of <0.1 kcal/mol, heating with C_α restrained to 300 K at intervals of 75 K, equilibration with C_α restrained for 100 ps, equilibration with no restraints for 600 ps, followed by 32 ns of the production run, in which the first ∼2 ns was the time required for the potential energy to stabilize and is not included in the analysis. From the resulting 30 ns MD trajectories, representative conformations of *Toxoplasma*, *Plasmodium*, and *Leishmania* α-tubulin were extracted every 2.5 ns for use in the AutoDock 3.0 docking simulations.[19]

Docking of Ligands. Flexible docking of all ligands was carried out over the entire α-tubulin structure using the adaptive Lamarckian genetic algorithm in AutoDock 3.0.[19] During the molecular docking runs, the macromolecule structures were kept rigid; therefore, using multiple structures of the macromolecule allows sampling of the side chain and backbone conformations and, thereby, captures some flexibility of the protein.[20] Fifty docking runs were performed for each α-tubulin conformation, using a grid spacing of 0.2 Å, a starting population size of 200, 25 million energy evaluations, a mutation rate of 0.07, a crossover rate of 0.8, and 600 iterations of Solis and Wets local search. The 600 bound ligand predictions resulting from the docking simulations were clustered on the basis of a root-mean-square deviation of 2.5 Å from the lowest docked energy conformation of the ligand. The site of the largest cluster with the lowest energy was selected as the active site of the ligand on α-tubulin, with the binding mode of the dinitroaniline being that of the lowest energy complex from this largest top cluster.

Parametrization of Compound 3. The molecular geometry of **3** was optimized with ab initio Hartree−Fock calculations, and the Merz−Singh−Kollman CHELPG style atom-centered point charges were derived with the HF/6-31G* basis set using Gaussian 98 (Gaussian Inc., Pittsburgh, PA). The bond-stretching, angle-bending, and torsional force field parameters for the sulfanilamide core and the nitro groups of **3** were taken from the MM3 force field,[21] whereas the Lennard−Jones force field parameters were adapted from the CHARMM22 force field parameters for proteins.[22] All bonded and Lennard−Jones force field parameters for the aryl ring at the *N1* nitrogen of the sulfanilamide and the alkane tail parameters were directly taken from the CHARMM22 force field parameters for proteins and the CHARMM27 force field parameters for lipids.[22,23] Having the force field parameters of the ligand, *Leishmania* α-tubulin in complex with **3** was subsequently simulated for 30 ns under the identical conditions used for the *Leishmania* apo structure.

Alignment of α-Tubulin Sequences. The amino acid residues that are conserved between plant and protozoan α-tubulin but are different from those found in mammalian and fungal α-tubulin were determined by performing multiple sequence alignment using ClustalW.[24] The α-tubulin sequences of the various species used in the alignment with accession codes in parentheses were *Zea mays* (CAD20822), *Eleusine indica* (CAA06619), *Toxoplasma gondii* (AAA30145), *Plasmodium* falciparum (CAA34101), *Leishmania* major (CAJ02501), *Trypanosoma brucei* (CAJ16366), *Sus scrofa* (P02550), *Homo sapiens* (NP_006073), *Saccharomyces cerevisiae* (NP_013625), and *Emericella nidulans* (P24634). The full alignment is shown in the Supporting Information.

Results

Docking of Dinitroanilines to Parasitic α-Tubulin. From the docking simulations of ligands **1**−**3** to multiple conformations of *T. gondii*, *P. falciparum*, and *L. major* α-tubulin, a consensus binding site for the dinitroanilines on parasitic α-tubulin was identified. This active site is located beneath the H1−S2 loop and is formed by the residues (based on the *Leishmania* sequence) of strand S1 (Arg2, Glu3, Ala4, Ile5, Cys6), helix H1 (Cys20, Trp21, Phe24), the H1−S2 loop (His28, Met36, Asp39, Lys40, Cys41, Ile42, Asp47, Pro63, Arg64), strand S2 (Cys65), strand S4 (Met136), helix H7 (Val235, Ser236, Thr239, Ala240, Ser 241), and the T7 loop (Arg243, Phe244, Asp245). Figure 2 shows representative structures of **1**−**3** bound to *Toxoplasma*, *Plasmodium*, and *Leishmania* α-tubulin in the binding conformation predicted by the docking

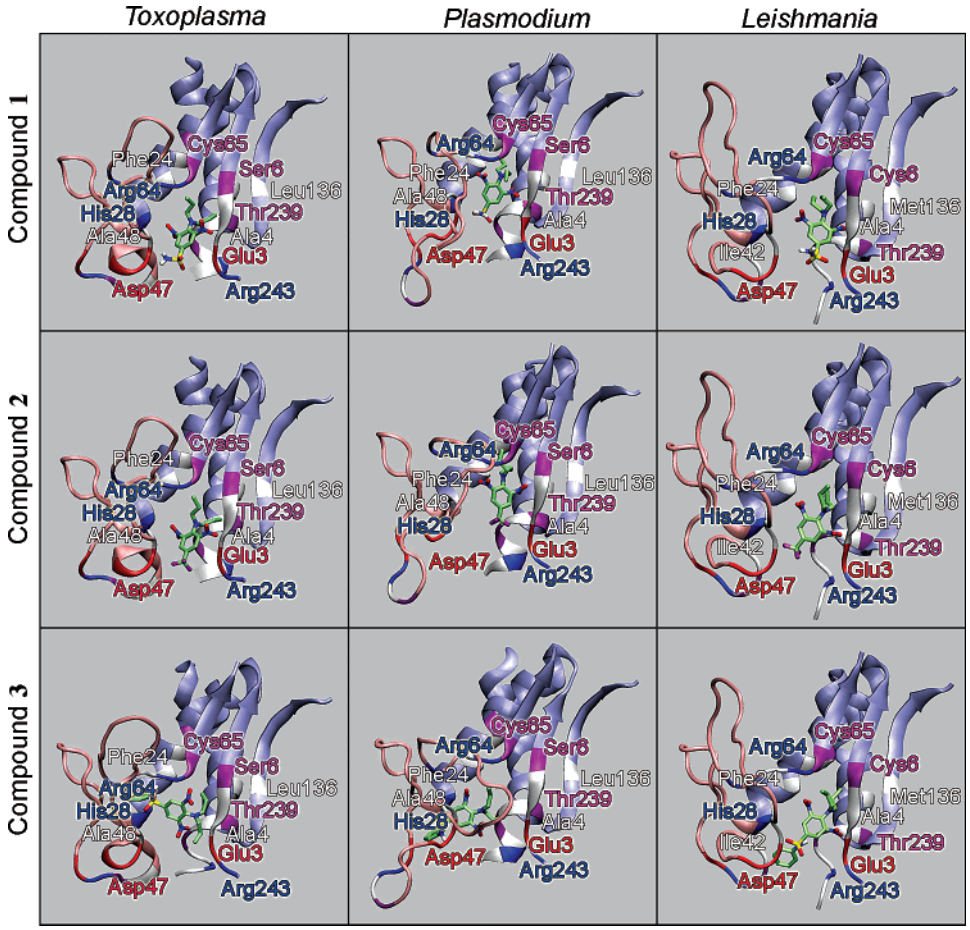

Figure 2. Representative structures of **1**, **2**, and **3** bound to *Toxoplasma gondii*, *Plasmodium falciparum* and *Leishmania major* α-tubulin as predicted by docking simulations. Key residues within 4 Å of the ligand are labeled, and the H1−S2 loop is colored pink. This and other molecular figures were created using VMD.[28]

Table 1. Two Largest Clusters from 600 Docking Runs with *Toxoplasma*, *Plasmodium*, and *Leishmania* α-Tubulin

compd	first cluster	second cluster	predicted Δ*G* (kcal/mol)
	Toxoplasma gondii		
1	53	42	−10.48
2	50	36	−9.96
3	16	9	−10.24
	Plasmodium falciparum		
1	23	14	−10.49
2	20	12	−9.88
3	24	15	−11.59
	Leishmania major		
1	53	32	−10.67
2	86	33	−9.88
3	58	47	−13.43

simulations. In this bound conformation, the hydrophobic alkane tails of the dinitroanilines orient toward the core of the protein, resulting in favorable interactions with residues Ala4, Ile5, Cys6, Cys20, Trp21, Phe24, Arg64, and Val235 (Figure 2). The sulfonamide headgroup of the dinitroanilines makes contact with the residues at the entrance to the binding site. More details and analysis of these ligand−protein interactions follow in the Discussion.

The docking results are summarized in Table 1. The top two clusters for each drug/tubulin combination were located at the binding site, although with slightly different conformations. The binding free energy predictions from AutoDock 3.0 can have errors as high as 2 kcal/mol; however, as observed in previous studies,[20] the docking of ligands to multiple protein structures taken from the MD trajectory leads to much more accurate free energy estimates. Likewise, here, we obtain the correct relative ordering of the inhibitors corresponding to their anti-parasitic activity, with **3** being the most potent against *Leishmania*, whereas **1** and **3** exhibit similar binding affinities for apicomplexan α-tubulin.

Effect on Tubulin Dynamics. Having identified the binding site of the dinitroanilines, MD simulations of the *Leishmania* α-tubulin alone and the *Leishmania* α-tubulin−**3** complex were performed in order to compare their dynamics and determine the molecular effect of the drug. To distinguish how protein flexibility is altered by the presence of the bound dinitroaniline, the rmsf of the C_α residues for the apo and holo structures were calculated (Figure 3A). To quantify any variation in dynamics, we found the difference between these rmsf plots, calculated the mean and standard deviation (σ) of this rmsf difference over the entire protein, and plotted the result in terms of the standard deviation from the mean (Figure 3B). The residues for which the C_α rmsf difference was at least 2σ from the mean were considered to be significant. These calculations reveal that the binding of **3** beneath the H1−S2 loop of α-tubulin severely restricts the flexibility of this loop, particularly affecting residues Asp39−Gly43 and Ser54−Ala58. Interestingly, long-range allosteric effects are also observed, resulting in a more than 50-fold enhancement in the flexibility of the M-loop residues Ser277−Tyr282 in the drug-bound protein complex.

The radius of gyration (R_g) of the α-tubulin binding site residues (those within 5 Å of the drug) were also examined for

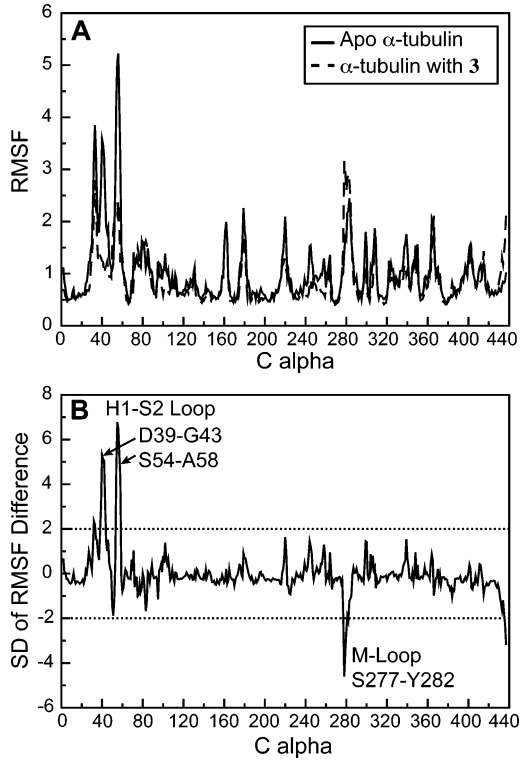

Figure 3. (A) Root-mean-square fluctuations of C_α residues of *Leishmania* apo and holo (bound with **3**) structures. (B) Difference between the apo and holo rmsf plots. Residues having C_α rmsf difference of at least 2σ from the mean (dotted line) are labeled.

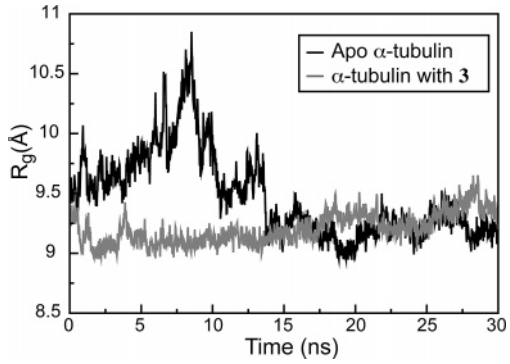

Figure 4. Radius of gyration of α-tubulin binding site residues within 5 Å of the drug for apo and holo (bound with **3**) structures.

both the apo and holo structures (Figure 4). In the apo form, the protein exhibits breathing motions, and the binding pocket of the protein changes between an open conformation (first half of the trajectory) and a closed conformation as a result of the high flexibility of the H1−S2 loop. This movement of the H1−S2 loop helps to maintain interprotofilament contacts and also enables easy access of the dinitroanilines into their binding site via the luminal surface of the MT. However, when **3** is bound at the active site, the interactions between the drug and the H1−S2 loop stabilize it in its closed conformation, giving a lower overall R_g. The waters in the binding pocket form a solvent network that links the nitro group oxygen atoms of **3** with Asp47 and Arg64 of α-tubulin. Hydrogen bonding is also observed between the sulfonamide oxygen of **3** and Cys41. In addition, the electrostatic and van der Waals interactions between the aromatic ring at the *N1* nitrogen of **3** and the α-tubulin residues His28, Met36, and Asp39−Ile42 keep the H1−S2 loop closer to the body of the drug-bound protein (Figure 5).

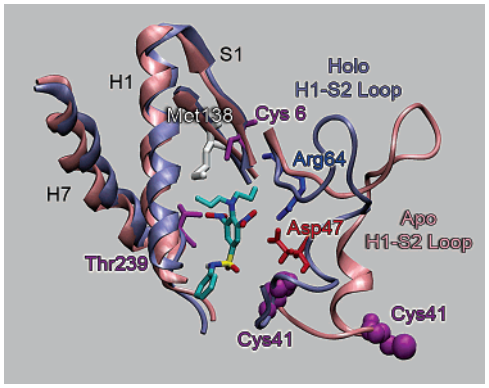

Figure 5. Movement of the H1−S2 loop (Ser38−Cys65) of α-tubulin−**3** complex (in blue) in the closed conformation relative to that in the open conformation observed for the apo structure (in pink). The binding site residues within 5 Å of the drug are labeled. The data shown is at 8.5 ns of the MD trajectory.

Design of Parasitic Microtubule Inhibitors. The analogues of **3** with hydroxymethyl (**4**; $\Delta G = -11.52$ kcal/mol), hydroxyethyl (**5**; $\Delta G = -12.34$ kcal/mol), or aminomethyl (**6**; $\Delta G = -12.10$ kcal/mol) moieties at the *N4* position exhibited weaker binding affinities compared to that of **3** ($\Delta G = -13.43$ kcal/mol), indicating that the presence of polar end groups and alkyl chains shorter than three carbon atoms at the *N4* nitrogen were not favored in the binding interactions. This is most likely due to the loss of favorable hydrophobic contacts between the dialkyl chains and the adjacent hydrophobic residues. This result agrees with the experimental observation that an increase in the length of the dialkyl chain at *N4* nitrogen improves anti-*Leishmania* activity.[12]

The aromatic nitro group of the sulfonamide has been implicated with host toxicity.[25] Our docking studies indicate that the replacement of both nitro groups by either carboxyl (**7**; $\Delta G = -13.97$ kcal/mol) or methyl ketone (**8**; $\Delta G = -14.54$ kcal/mol) moieties leads to stronger binding to *Leishmania* α-tubulin compared to that of **3**. The bound conformation of the drug indicates that a methyl ketone group would enhance hydrophobic contacts with α-tubulin residues Trp21, Phe24, and Phe244. In contrast, the dicyano analogue (**9**; $\Delta G = -13.47$ kcal/mol) has a similar binding affinity to **3** and has been found experimentally to be as equally active as **3** against both *Leishmania* tubulin assembly and parasite growth (Werbovetz, K. Personal communication). On the basis of free energy perturbation calculations, dinitroaniline **10** has a 1 kcal/mol more favorable binding free energy compared to that of **3**, indicating that a hydroxyl group is favored at the meta position of the phenyl ring at the *N1* nitrogen of the sulfonamide (see Supporting Information for details).

Discussion

In this work, MD simulations and molecular docking studies have been used to identify a single high-affinity binding site for **1**, **2**, and **3** on *Toxoplasma gondii*, *Plasmodium falciparum* and *Leishmania major* α-tubulin. The binding site is located beneath the H1−S2 loop and includes residues on helix H7 and on the T7 loop. Residues 52−62 in the H1−S2 loop of both α- and *β*-tubulin play an important role in stabilizing the MT. As observed in MD simulations of a MT fragment, these residues participate in noncovalent interactions with the M-loop residues 275−287 of the monomers in the neighboring protofilament (Mitra, A.; Sept, D. Unpublished data; Figure 6). The conformational stability of helix H7 is also important because it contacts both the GTPase domain and the activation domain.[26]

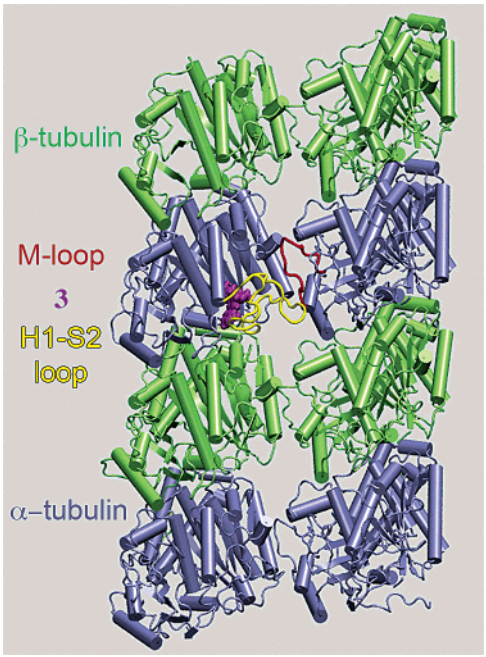

Figure 6. Location of the dinitroaniline binding site within the microtubule lattice. This is a view from the inside of the microtubule and suggests that dinitroanilines may disrupt the interaction of the H1−S2 and M loops, leading to microtubule instability.

Helix H7 is also connected to loop T7, which, along with helix H8, is involved in interdimer longitudinal contacts. Our results demonstrate that dinitroanilines lower the flexibility of the H1−S2 loop, and through its direct interaction with the ligand, the H1−S2 loop is pulled closer to the body of the α-tubulin, displacing it from the M-loop of the α-tubulin subunit in the neighboring protofilament. This result may in fact be compounded by the change in the flexibility of the M-loop that we observed. The combination of these two effects could lead to the disruption of lateral protofilament contacts and eventually cause MT disassembly.

Recent studies indicate that a few *Toxoplasma* α-tubulin mutations associated with resistance to **1** are located on helix 7 and its immediate proximity, on the H1−S2 loop and on the *β*-sheet formed by strands S1, S4, and S5.[16] Six of these 23 mutations (His28Gln, Leu136Phe, Ile235Val, Thr239Ile, Arg243Cys, and Arg243Ser) are of residues that have direct interactions with the ligand in the identified binding site. Furthermore, the Thr239Ile point mutation, which confers the highest resistance to **1** (5 μM), is located within 3 Å of the nitro group oxygen. The effect of the other mutants appears to be primarily allosteric in nature. This premise is supported by the fact that although the Ser165Ala mutation resulted in 2 μM resistance to **1** and the Ser165Ala/Thr239Ile double mutant exhibited >90 μM resistance,[16] Ser165 does not form a part of the dinitroaniline binding pocket and is located on strand S5 more than 10 Å away from Thr239.

Interestingly, although dinitroanilines disrupt plant and protozoan MTs, they are ineffective against mammalian and fungal tubulin. It would seem logical that some insight into this selectivity could be obtained by simple sequence alignment (Supporting Information); however, mapping the conserved plant and protozoan residues on the α-tubulin structure shows that these residues mainly cluster around the interior of the tubulin molecule and do not distinctly define a binding site. Most notably, the binding site residues identified in this study are not specific to plant and protozoan tubulin, but many are in fact conserved in fungi and mammals as well. Just as we observe long-range allosteric effects due to dinitroaniline binding, it seems evident that these nonlocal sequence differences must likewise affect the conformation, dynamics, and/or access to the H1−S2 binding site. This hypothesis is supported by the fact that similar dynamics and docking studies using bovine α-tubulin resulted in a 50-fold weaker binding affinity and no consensus binding site, in agreement with experimental findings.[16]

Recently, Blume and co-workers[27] analyzed the change in the surface electrostatic potential between wild-type *Eleusine indica* α-tubulin and the corresponding resistant Thr239Ile α-tubulin point mutant and proposed a binding site including residues Arg239, Arg243, Asp251, Val252, and Asn253 (and partly Cys4, His8, Leu136, and Phe138). Although some residues, namely, Cys4, Leu136, Thr239, and Arg243, of their active site overlap with the those determined in this study and the binding sites are in close proximity, the two predictions are distinct. In their study, the dinitroanilines bind at the dimer interface, whereas in this work, the active site is directly behind the H1−S2 loop and primarily destabilizes the lateral contacts between protofilaments, along with disrupting longitudinal interdimer contacts, leading to microtubule disassembly.

One shortfall of current docking methodologies is that the response of the macromolecule to the bound ligand is not taken into account. In this case, we have overcome this difficulty by performing MD simulations of the α-tubulin−**3** complex, allowing the protein and the drug to respond to each other. This results in a snug fit of the aromatic ring at the *N1* nitrogen of the compound with the α-tubulin residues Phe24, His28, Met36, Asp39−Ile42, and Ser241−Asp245 that form the entrance of the binding pocket. The aromatic ring at the *N1* nitrogen and the His28 imidazole ring also interact through ring-stacking interactions. Hydrogen bonding is also observed between the *N1* nitrogen of the sulfonamide and Ala240, as well as between the sulfonamide oxygen and Cys41 (on the H1−S2 loop). The nitro group oxygen atoms have electrostatic interactions with Glu3 (on strand S1), Thr239 (on helix H7), and Arg243 (on T7 loop), whereas hydrogen bonding is observed between the nitro group oxygen and Ala4. Interestingly, the second nitro group oxygen has no direct interactions with α-tubulin, but is linked by the solvent network to the salt-bridge between Asp47 and Arg64. Finally, unfavorable steric interactions between the ligand and the protein may occur if the hydrogen atoms of the phenyl ring are substituted either by a polar group larger than a hydroxyl group or by alkyl side chains, consistent with experimental observations.[12] It is hopeful that these findings provide some insight for future SAR based design of dinitroaniline analogues.

Acknowledgment. We thank Naomi Morrissette and Karl Werbovetz for experimental data, many useful discussions, and comments on the manuscript. We acknowledge financial support from the National Institutes of Health Grant R01-AI-062021.

Supporting Information Available: Complete α-tubulin sequence alignment and details of the free energy perturbation calculations. This material is available free of charge via the Internet at http://pubs.acs.org.

References

(1) Hugdahl, J. D.; Morejohn, L. C. Rapid and reversible high-affinity binding of the dinitroaniline herbicide oryzalin to tubulin from Zea mays L. *Plant Physiol.* **1993**, *102*, 725−740.
(2) Morejohn, L. C.; Bureau, T. E.; Mole-Bajer, J.; Bajer, A. S.; Fosket, D. E. Oryzalin, a dinitroaniline herbicide, binds to plant tubulin and inhibits microtubule polymerization in vitro. *Planta* **1987**, *172*, 252−264.

(3) Murthy, J. V.; Kim, H. H.; Hanesworth, V. R.; Hugdahl, J. D.; Morejohn, L. C. Competitive-inhibition of high-affinity oryzalin binding to plant tubulin by the phosphoric amide herbicide amiprophos-methyl. *Plant Physiol.* **1994**, *105*, 309−320.
(4) Bogitsh, B. J.; Middleton, O. L.; Ribeiro-Rodrigues, R. Effects of the antitubulin drug trifluralin on the proliferation and metacyclogenesis of *Trypanosoma cruzi* epimastigotes. *Parasitol. Res.* **1999**, *85*, 475−480.
(5) Traub-Cseko, Y. M.; Ramalho-Ortigao, J. M.; Dantas, A. P.; de Castro, S. L.; Barbosa, H. S.; Downing, K. H. Dinitroaniline herbicides against protozoan parasites: the case of *Trypanosoma cruzi*. *Trends Parasitol.* **2001**, *17*, 136−141.
(6) Bhattacharya, G.; Salem, M. M.; Werbovetz, K. A. Antileishmanial dinitroaniline sulfonamides with activity against parasite tubulin. *Bioorg Med. Chem. Lett.* **2002**, *12*, 2395−2398.
(7) Chan, M. M.; Fong, D. Inhibition of leishmanias but not host macrophages by the antitubulin herbicide trifluralin. *Science* **1990**, *249*, 924−926.
(8) Chan, M. M.; Tzeng, J.; Emge, T. J.; Ho, C. T.; Fong, D. Structure−function analysis of antimicrotubule dinitroanilines against promastigotes of the parasitic protozoan Leishmania mexicana. *Antimicrob. Agents Chemother.* **1993**, *37*, 1909−1913.
(9) Nath, J.; Schneider, I. Antimalarial effects of the antitubulin herbicide trifluralin: studies in Plasmodium-falciparum. *Clin. Res.* **1992**, *40*, A331−A331.
(10) Stokkermans, T. J.; Schwartzman, J. D.; Keenan, K.; Morrissette, N. S.; Tilney, L. G.; Roos, D. S. Inhibition of Toxoplasma gondii replication by dinitroaniline herbicides. *Exp. Parasitol.* **1996**, *84*, 355−370.
(11) Chan, M. M.; Triemer, R. E.; Fong, D. Effect of the anti-microtubule drug oryzalin on growth and differentiation of the parasitic protozoan Leishmania mexicana. *Differentiation* **1991**, *46*, 15−21.
(12) Bhattacharya, G.; Herman, J.; Delfin, D.; Salem, M. M.; Barszcz, T.; Mollet, M.; Riccio, G.; Brun, R.; Werbovetz, K. A. Synthesis and antitubulin activity of N1- and N4-substituted 3,5-dinitro sulfanilamides against African trypanosomes and Leishmania. *J. Med. Chem.* **2004**, *47*, 1823−1832.
(13) Werbovetz, K. A.; Sackett, D. L.; Delfin, D.; Bhattacharya, G.; Salem, M.; Obrzut, T.; Rattendi, D.; Bacchi, C. Selective antimicrotubule activity of N1-phenyl-3,5-dinitro-N4,N4-di-*n*-propylsulfanilamide (GB-II-5) against kinetoplastid parasites. *Mol. Pharmacol.* **2003**, *64*, 1325−1333.
(14) Fowler, R. E.; Fookes, R. E.; Lavin, F.; Bannister, L. H.; Mitchell, G. H. Microtubules in Plasmodium falciparum merozoites and their importance for invasion of erythrocytes. *Parasitology* **1998**, *117*, 425−433.
(15) Kaidoh, T.; Nath, J.; Fujioka, H.; Okoye, V.; Aikawa, M. Effect and localization of trifluralin in Plasmodium falciparum gametocytes: an electron microscopic study. *J. Eukaryot. Microbiol.* **1995**, *42*, 61−64.
(16) Morrissette, N. S.; Mitra, A.; Sept, D.; Sibley, L. D. Dinitroanilines bind alpha-tubulin to disrupt microtubules. *Mol. Biol. Cell* **2004**, *15*, 1960−1968.
(17) Vriend, G. WHAT IF: a molecular modeling and drug design program. *J. Mol. Graph.* **1990**, *8*, 52−56.
(18) Kale, L.; Skeel, R.; Bhandarkar, M.; Brunner, R.; Gursoy, A.; Krawetz, N.; Phillips, J.; Shinozaki, A.; Varadarajan, K.; Schulten, K. NAMD2: Greater scalability for parallel molecular dynamics. *J. Comput. Phys.* **1999**, *151*, 283−312.
(19) Morris, G. M.; Goodsell, D. S.; Halliday, R. S.; Huey, R.; Hart, W. E.; Belew, R. K.; Olson, A. J. Automated docking using a Lamarckian genetic algorithm and empirical binding free energy function. *J. Comput. Chem.* **1998**, *19*, 1639−1662.
(20) Mitra, A.; Sept, D. Localization of the antimitotic peptide and depsipeptide binding site on beta-tubulin. *Biochemistry* **2004**, *43*, 13955−13962.
(21) Allinger, N. L.; Yuh, Y. H.; Lii, J. H. Molecular mechanics: the Mm3 force-field for hydrocarbons 0.1. *J. Am. Chem. Soc.* **1989**, *111*, 8551−8566.
(22) MacKerell, A. D.; Bashford, D.; Bellott, M.; Dunbrack, R. L.; Evanseck, J. D.; Field, M. J.; Fischer, S.; Gao, J.; Guo, H.; Ha, S.; Joseph-McCarthy, D.; Kuchnir, L.; Kuczera, K.; Lau, F. T. K.; Mattos, C.; Michnick, S.; Ngo, T.; Nguyen, D. T.; Prodhom, B.; Reiher, W. E.; Roux, B.; Schlenkrich, M.; Smith, J. C.; Stote, R.; Straub, J.; Watanabe, M.; Wiorkiewicz-Kuczera, J.; Yin, D.; Karplus, M. All-atom empirical potential for molecular modeling and dynamics studies of proteins. *J. Phys. Chem. B* **1998**, *102*, 3586−3616.
(23) Feller, S. E.; MacKerell, A. D. An improved empirical potential energy function for molecular simulations of phospholipids. *J. Phys. Chem. B* **2000**, *104*, 7510−7515.
(24) Pearson, W. R. Rapid and sensitive sequence comparison with Fastp and Fasta. *Methods Enzymol.* **1990**, *183*, 63−98.
(25) Berman, J. D. Human leishmaniasis: clinical, diagnostic, and chemotherapeutic developments in the last 10 years. *Clin. Infect. Dis.* **1997**, *24*, 684−703.
(26) Amos, L. A. Microtubule structure and its stabilisation. *Org. Biomol. Chem.* **2004**, *2*, 2153−2160.
(27) Blume, Y. B.; Nyporko, A. Y.; Yemets, A. I.; Baird, W. V. Structural modeling of the interaction of plant alpha-tubulin with dinitroaniline and phosphoroamidate herbicides. *Cell. Biol. Int.* **2003**, *27*, 171−174.
(28) Humphrey, W.; Dalke, A.; Schulten, K. VMD: Visual molecular dynamics. *J. Mol. Graphics* **1996**, *14*, 33−38.

JM060472+